

NASA/TM–20210016872



Detect-and-Avoid Safety and Operational Suitability Analysis using an Electro-Optical/Infrared Sensor Model

*Christine Serres, Bilal Gill, Matthew W. M. Edwards
Lincoln Laboratory, Massachusetts Institute of Technology, Lexington, Massachusetts*

*M. Gilbert Wu
Ames Research Center, Moffett Field, California*

March 2021

NASA STI Program . . . in Profile

Since its founding, NASA has been dedicated to the advancement of aeronautics and space science. The NASA scientific and technical information (STI) program plays a key part in helping NASA maintain this important role.

The NASA STI program operates under the auspices of the Agency Chief Information Officer. It collects, organizes, provides for archiving, and disseminates NASA's STI. The NASA STI program provides access to the NTRS Registered and its public interface, the NASA Technical Reports Server, thus providing one of the largest collections of aeronautical and space science STI in the world. Results are published in both non-NASA channels and by NASA in the NASA STI Report Series, which includes the following report types:

- **TECHNICAL PUBLICATION.** Reports of completed research or a major significant phase of research that present the results of NASA Programs and include extensive data or theoretical analysis. Includes compilations of significant scientific and technical data and information deemed to be of continuing reference value. NASA counter-part of peer-reviewed formal professional papers but has less stringent limitations on manuscript length and extent of graphic presentations.
- **TECHNICAL MEMORANDUM.** Scientific and technical findings that are preliminary or of specialized interest, e.g., quick release reports, working papers, and bibliographies that contain minimal annotation. Does not contain extensive analysis.
- **CONTRACTOR REPORT.** Scientific and technical findings by NASA-sponsored contractors and grantees.

- **CONFERENCE PUBLICATION.** Collected papers from scientific and technical conferences, symposia, seminars, or other meetings sponsored or co-sponsored by NASA.
- **SPECIAL PUBLICATION.** Scientific, technical, or historical information from NASA programs, projects, and missions, often concerned with subjects having substantial public interest.
- **TECHNICAL TRANSLATION.** English-language translations of foreign scientific and technical material pertinent to NASA's mission.

Specialized services also include organizing and publishing research results, distributing specialized research announcements and feeds, providing information desk and personal search support, and enabling data exchange services.

For more information about the NASA STI program, see the following:

- Access the NASA STI program home page at <http://www.sti.nasa.gov>
- E-mail your question to help@sti.nasa.gov
- Phone the NASA STI Information Desk at 757-864-9658

NASA/TM–20210016872



Detect-and-Avoid Safety and Operational Suitability Analysis using an Electro-Optical/Infrared Sensor Model

*Christine Serres, Bilal Gill, Matthew W. M. Edwards
Lincoln Laboratory, Massachusetts Institute of Technology, Lexington, Massachusetts*

*M. Gilbert Wu
Ames Research Center, Moffett Field, California*

National Aeronautics and
Space Administration

Ames Research Center
Moffett Field, California 94035

March 2021

Table of Contents

TABLE OF CONTENTS 1

LIST OF ABBREVIATIONS 3

1 INTRODUCTION 4

2 EO/IR SENSOR MODEL..... 4

2.1 BEARING AND ELEVATION ERROR..... 5

2.2 BEARING AND ELEVATION RATE ERROR 5

2.3 RANGE ERROR 5

2.4 RANGE-RATE ERROR MODEL..... 6

2.5 DETECTION RANGE..... 6

3 ENCOUNTER SET 6

4 ANALYSIS SETUP 7

5 SIMULATION SETUP 9

6 METRICS 12

7 RESULTS..... 14

7.1 SAFETY METRICS..... 14

7.1.1 RISK RATIO 14

7.1.2 LOWC RATIO 15

7.2 OPERATIONAL SUITABILITY METRICS..... 15

7.2.1 SPLIT ALERT PROBABILITY 15

7.2.2 EXPECTED NUMBER OF SPLIT ALERTS..... 17

7.2.3 REVERSAL PROBABILITY..... 17

7.2.4 EXPECTED NUMBER OF REVERSALS 17

7.2.5 PILOT WORKLOAD 18

7.2.6 SYSTEM OPERATING CHARACTERISTIC (ALERT RATIO AND RISK RATIO) 19

7.3 ADDITIONAL ANALYSES..... 20

7.3.1	INCREASING ANGULAR RATE ERROR TIME CORRELATION	20
7.3.2	INCREASING RANGE AND RANGE-RATE ERROR TIME CORRELATION.....	20
8	CONCLUSIONS AND FUTURE WORK.....	21
	REFERENCES.....	22

List of Abbreviations

ADS-B	Automatic Dependent Surveillance - Broadcast
AGL	Above Ground Level
ATAR	Air-To-Air Radar
ATC	Air Traffic Controller
DAA	Detect and Avoid
DAIDALUS	Detect and Avoid Alerting Logic for Unmanned Systems
DWC	DAA Well Clear
EO/IR	Electro Optical or Infra-Red
FAA	Federal Aviation Administration
IFR	Instrument Flight Rules
KTAS	Knots True Airspeed
LoWC	Loss of DAA Well Clear
MOPS	Minimum Operational Performance Standards
NAS	National Airspace System
NASA	National Aeronautics and Space Administration
NM	Nautical Mile(s)
NMAC	Near Mid Air Collision
NTRS	NASA Technical Reports Server
PDF	Probability distribution function
RTCA, Inc.	Radio Technical Commission for Aeronautics
SC	Special Committee
STI	NASA Scientific and Technical Information
SUM	Sensor Uncertainty Mitigation
SWaP	Size, Weight and Power
TCAS	Traffic Alert and Collision Avoidance System
TM	Technical Memorandum
UA	Unmanned Aircraft
UAS	Unmanned Aircraft Systems
VLOS	Visual Line of Sight
WG	Working Group

1 INTRODUCTION

Detect-and-avoid (DAA) systems provide surveillance, alerting, and maneuver guidance that are critical to unmanned aircraft systems' (UAS) ability to maintain separation from hazards such as manned aircraft and other unmanned aircraft. The last decade has seen significant progress in the development of requirements of DAA systems, spearheaded by RTCA Special Committee 228 (SC-228) and subsequently followed by other standards organizations in both the US and other countries. SC-228's development of DAA requirements assumes the UAS follows the instrument flight rules (IFR) and has a remote pilot or operator in the loop. The DAA's surveillance systems must detect both cooperative and non-cooperative air traffic. Non-cooperative traffic are aircraft that do not have a broadcasting transponder. According to SC-228's latest Minimum Operational Performance Standards (MOPS) for DAA, versioned as DO-365B [1], DAA systems use onboard and/or ground surveillance systems to detect traffic. The alerting and guidance functions alert the pilot/operator in the loop of potential hazards, such as intruder aircraft, and provide maneuver solutions which help the pilot/operator avoid or mitigate observed hazards. Pilots/operators should coordinate with air traffic control (ATC) for a maneuver if time permits.

Electro-Optical/Infra-Red sensors (EO/IR) are low size, weight, and power (SWaP) airborne sensors potentially suitable for DAA surveillance. EO/IR sensors operate in both visible or infrared wavelengths and provide situation awareness in both day and night conditions. Under favorable atmospheric conditions and suitable operational assumptions, EO/IR sensors can fulfill the performance requirements of a non-cooperative DAA sensor. Compared to the air-to-air-radar (ATAR), another non-cooperative sensor for which requirements have been researched and defined in SC-228's DO-366A, EO/IR sensors' performance varies with a distinct set of environmental parameters. EO/IR sensors also exhibit distinct error characteristics. While EO/IR sensors provide comparable or superior angular accuracy of an intruder aircraft's positions, its range and range rate estimates are subject to larger errors than provided by ATAR measurements. The impact of EO/IR sensors' error characteristics on the DAA system's performance is not well understood and has been a potential concern for EO/IR sensors' applicability to DAA systems. Sensitivity of DAA systems' performance to EO/IR sensors' error parameters needs to be investigated before requirements of EO/IR sensors for DAA can be confidently defined.

This report describes a modeling and simulation study that directly supports the development of the MOPS for EO/IR sensors. An EO/IR sensor model derived from flight test data is applied to generate noisy tracks from truth data as input to a reference DAA alerting and guidance algorithm. DAA safety and operational suitability metrics are computed from simulation of a large number of representative DAA encounters. The reference DAA alerting and guidance algorithm, coupled to a pilot response model, are applied to compute these metrics. The UA equipped with the DAA system is assumed to fly like a fixed-wing aircraft at a speed between 40 and 110 kts. This study specifically assesses the sensitivity of these metrics to sensor measurement errors and detection range.

This report is organized as follows: Section 2 describes the EO/IR sensor model. Section 3 describes the encounter set used for the analysis. Section 4 describes the analysis approach. Section 5 describes the simulation setup. Section 6 describes the safety and operational suitability metrics computed in this analysis. Section 7 presents the results, and Section 8 concludes this report.

2 EO/IR SENSOR MODEL

The EO/IR sensor model used in this analysis was based on a white paper published by Safran Electronics & Defense [2]. All references to an EO/IR sensor in this paper refer to the minimum performance EO/IR sensor model described in the white paper. Although the EO/IR sensor model was developed by Safran, the model is intended to be generic. The key characteristics of the EO/IR sensor model as stated in the Safran white paper are described in this section.

The EO/IR sensor model emulates errors of bearing, elevation, bearing rate, elevation rate, range, and range-rate measurements or estimates from the ownship to the intruder. An EO/IR sensor cannot natively detect range and range-rate, and the sensor must perform additional processing to extract that information. The following sub-sections describe each error parameter in detail.

2.1 Bearing and Elevation Error

The bearing and elevation errors are modeled as Gaussian white noise. The standard deviation of the bearing and elevation errors is:

$$\sigma_a = 0.001 \text{ rad}$$

The bearing and elevation errors are not time correlated.

2.2 Bearing and Elevation Rate Error

The bearing and elevation rate errors are modeled as Gauss-Markov noise [3]. The standard deviation of the bearing and elevation rate errors is:

$$\sigma_{ar} = 0.0014 \text{ rad/s}$$

The time correlation is dependent on the sensor sampling frequency. The Safran white paper defines the time correlation to be approximately 10 samples. In the simulation, the EO/IR sensor model was executed at 10 Hz, so the resulting time correlation was 1 second.

2.3 Range Error

The range estimation accuracy is dependent on the intruder type and the true range. For a Cessna type aircraft, the range error is the following:

$$\begin{aligned} \varepsilon_r(R) &= \mu_r(R) + CRE(R, t) \\ \mu_r(R) &= 50 - 0.15 \cdot \text{MAX}(0; R - 3000) \\ \sigma_r(R) &= 0.03 \cdot R \end{aligned}$$

where ε_r is the total range error, μ_r is the range bias error, σ_r is the range error standard deviation, and R is the true range in ft. $CRE(R, t)$ is colored random error as a function of range R and timestep t :

$$CRE(R, t) = \sigma_r(R) \cdot \text{randn}(1) \sqrt{1 - (e^{-\frac{dt}{\tau}})(e^{-\frac{dt}{\tau}})} + CRE(t - dt)e^{-\frac{dt}{\tau}}$$

The function $\text{randn}(1)$ returns a number drawn from a standard normal distribution. The correlation time parameter (τ) for range error is set to 5 seconds and dt is 0.1 seconds. The initial value of the colored random error is:

$$CRE(R, 0) = \sigma_r(R) \cdot \text{randn}(1).$$

Figure 1 shows plots of the range bias, random range error, and total range error from one execution of the model. For a representative range of 4,000 m (~13,000 ft), the EO/IR range error is ~1000 ft, considerably larger than the standard range error of 70 ft required for an airborne radar for DAA [4].

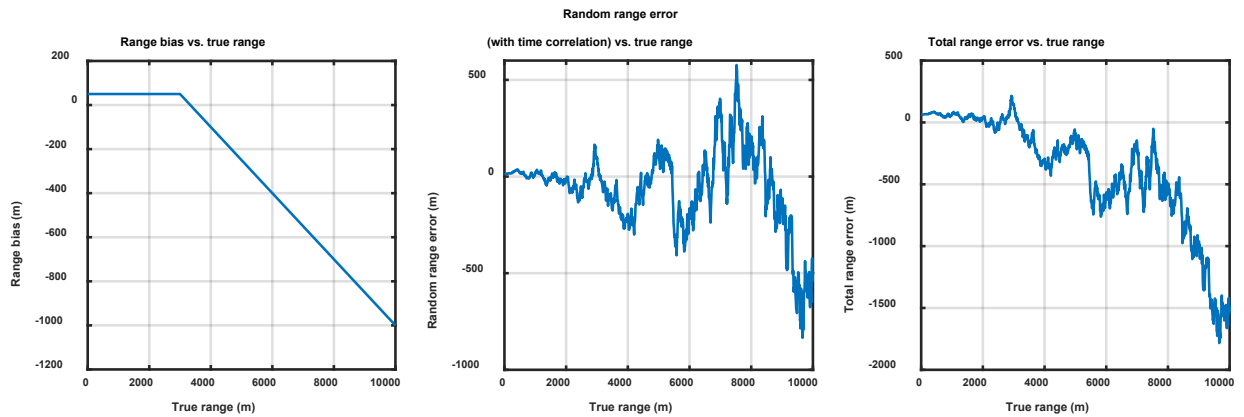


Figure 1 Range estimation error plots

2.4 Range-rate Error Model

The range-rate error is modeled by Gauss-Markov noise. The standard deviation of the range-rate error is:

$$\sigma_{rr}(RR) = 0.05 \cdot RR$$

Where RR is the true range rate. The EO/IR sensor needs 5 seconds since the time of first detection to start outputting a valid range-rate. The time correlation for the range-rate is 2 seconds.

For a representative range rate of 250 kts, σ_{rr} is about 20 ft/s. However, Safran indicated σ_{rr} beyond 2 NM is better represented by

$$\sigma_{rr}(RR) = 0.20 \cdot RR,$$

which would lead to 80 ft/s error. These values are considerably larger than the standard range rate error of 10 ft/s required for an airborne radar for DAA [4]. For this analysis, the smaller σ_{rr} of 20 ft/s was applied throughout the range since information of the worse range rate error beyond 2 NM, as stated in Safran, was not available.

2.5 Detection Range

The baseline detection range is set to 2.5 NM, a candidate range requirement for the low-speed UAS operations considered. This value was found in previous fast-time [4] and human-in-the-loop simulations [5] to be the minimum surveillance range that does not impact safety metrics in the presence of little or no sensor errors. For medium to large intruder aircraft such as the Cessna 172 and Beechcraft B200, the detection range of 2.5 NM is comfortably achievable by current EO/IR technologies under favorable or suitable atmospheric conditions.

3 ENCOUNTER SET

To evaluate the performance of a DAA system given EO/IR sensor measurements of intruder aircraft under various encounter situations, one million uncorrelated pairwise encounters that each has trajectories of one UAS and one noncooperative intruder were created as test points. Uncorrelated encounters model situations where intervention from Air Traffic Control (ATC) is unlikely, and aircraft can blunder into close proximity. The UAS trajectory was sampled from NASA's Airspace Concept Evaluation System UAS

database [6], and the intruder trajectory was sampled from MIT Lincoln Laboratory’s Uncorrelated Encounter Model [7]. The Uncorrelated Encounter Model is derived from radar data of observed aircraft operations under visual flight rules in the National Airspace System.

NASA’s UAS mission flights consist of different mission types, including aerial imaging and mapping, law enforcement, and air quality monitoring. The trajectories cover the entire continental US. Since EO/IR sensors’ surveillance range may only be sufficient for supporting medium to low closure rate encounters’ alerting times, only UAS trajectories at or below 110 KTAS were included. These trajectories were modeled by RQ-7 AAI Shadow B and MQ-19 AAI Aerosonde. The models used for these aircraft are similar to those in the Eurocontrol Base of Aircraft Data [8].

The intruder trajectory is sampled from the Uncorrelated Encounter Model randomly around the ownship trajectory that is statistically representative of noncooperative trajectories. Each encounter is specified by the initial positions and orientations of the two aircraft in the simulation and the nominal dynamic maneuvers that may occur leading up to the time of closest approach. The nominal dynamic maneuvers refer to horizontal or vertical accelerations observed in the trajectories of the UAS and the intruder aircraft.

Filters were applied to the ownship and intruder speeds and altitudes such that the dynamics of the sampled trajectories are within the bounds for low SWaP UAS and the intruders they are expected to encounter. The low SWaP UAS speeds are constrained between 40 and 110 KTAS, and the intruder speeds range from 0 to 170 KTAS—the 95th percentile speed for non-cooperative intruders in the Uncorrelated Encounter Model. The SC-228 committee agreed that 170 KTAS is the upper bound for non-cooperative intruders that need to be considered for modeling and simulation work. The encounters occur at altitudes between 500 ft above ground level and 11,000 ft mean sea level (MSL) in airspace classes E and G. Although Class E only extends to 10,000 ft MSL when it is adjacent to class B or class C airspace, altitudes up to 10,999 ft were included to represent low SWAP UAS missions that are flown slightly above 10,000 ft. The resulting altitude and speed distributions are shown in Figure 2.

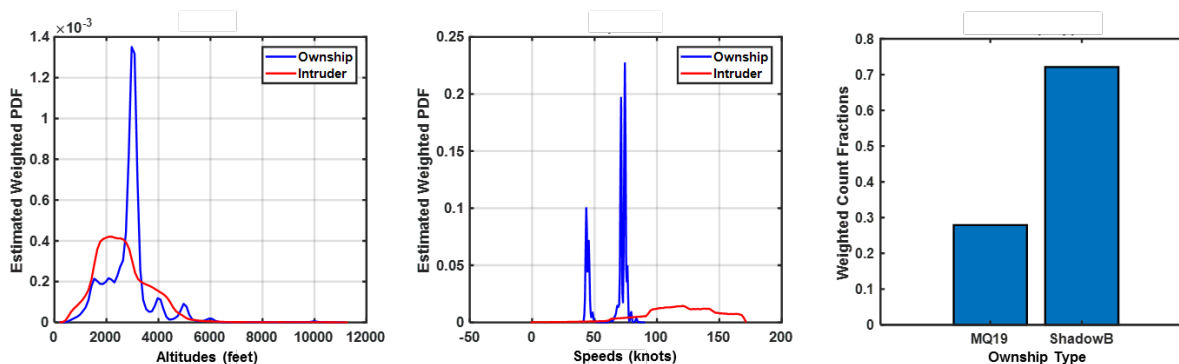


Figure 2 Encounter Characteristics

4 ANALYSIS SETUP

This analysis was set up so that the effect of individual EO/IR parameters on safety and operational suitability metrics could be isolated. This was done by taking the baseline EO/IR sensor model configuration and sweeping its parameters to be less than and greater than their baseline values. In the end-to-end simulation (to be explained in Section 5), the ownship was equipped with an EO/IR sensor with the modified parameters. EO/IR sensor measurements of the intruder were input to Detect and Avoid Alerting Logic for Unmanned Systems (DAIDALUS) version 1.0, a reference Detect-And-Avoid (DAA)

algorithm [9] for the DAA MOPS. The simulated ownship uses DAIDALUS-computed alerts and maneuver guidance to perform maneuvers to remain well clear from the intruder. The simulation was first run with no DAA maneuvers performed by the ownship to get baseline, open-loop values for the metrics; this is referred to as the nominal run. After that, the end-to-end, closed-loop simulation was run for the one million encounters per sensor configuration so that the aggregate metrics could be collected and analyzed.

Initially, the five parameters that were swept were range bias, angular (bearing and elevation) rate error, detection range, range error, and range-rate error. Angular errors from EO/IR are small and typically in the range of 0.001 radian as indicated in Section 2.1, These errors are considered well below the acceptable threshold for DAA and therefore were not examined.

Table 1 shows the different configurations that were analyzed. Configuration 1 turns off all measurement errors (including angular error) and detection range limits and serves as an “ideal” configuration. Configuration 2 is the default configuration as all of the parameters are equal to their baseline values. Configuration 3 turns off the range bias. The range bias was disabled for every subsequent run because the effect of the range bias on the metrics was found to be minimal and secondary. Configuration 4 applies the baseline errors by increasing DAIDALUS’s vertical alerting threshold from 450 ft to 4000 ft (see Section 5 for more detail about DAIDALUS). This is similar to the DO-365 MOPS recommendation for encounters with noncooperative aircraft. Configurations 5 through 8 swept through the angular rate error, configurations 9 through 13 swept through the detection range, configurations 14 through 18 swept through the range error, configurations 19 through 23 swept through the range-rate error, and configurations 24 through 26 swept through the range and range-rate errors together.

Table 1 Analysis Configurations

#	Range bias	Angular rate error %	Detection Range (NM)	Range error %	Range-rate error %	Comment
1	Off	0%	Infinite	0%	0%	Benchmark
2	On	100%	2.5	100%	100%	
3	Off	100%	2.5	100%	100%	
4	Off	100%	2.5	100%	100%	Increased vertical separation buffer to 4000 ft
5	Off	50%	2.5	100%	100%	
6	Off	75%	2.5	100%	100%	
7	Off	125%	2.5	100%	100%	
8	Off	150%	2.5	100%	100%	
9	Off	100%	1	100%	100%	
10	Off	100%	1.5	100%	100%	
11	Off	100%	2	100%	100%	
12	Off	100%	3	100%	100%	
13	Off	100%	4	100%	100%	

14	Off	100%	2.5	50%	100%	
15	Off	100%	2.5	75%	100%	
16	Off	100%	2.5	125%	100%	
17	Off	100%	2.5	150%	100%	
18	Off	100%	2.5	400%	100%	
19	Off	100%	2.5	100%	50%	
20	Off	100%	2.5	100%	75%	
21	Off	100%	2.5	100%	125%	
22	Off	100%	2.5	100%	150%	
23	Off	100%	2.5	100%	400%	
24	Off	100%	2.5	400%	400%	
25	Off	100%	2.5	800%	800%	
26	Off	100%	2.5	1200%	1200%	

5 SIMULATION SETUP

Figure 3 shows the CASSATT (Collision Avoidance System Safety Assessment Tool) end-to-end simulation architecture used for this analysis. CASSATT is a fast-time Monte Carlo simulation framework developed by MIT Lincoln Laboratory that takes encounter model data as an input and simulates aircraft motion for an ownship and intruder. For this analysis, the input to CASSATT was an encounter, sampled from one million encounters described in Section 3, that consisted of roughly 3-minute truth trajectories for an ownship aircraft and an intruder aircraft. The encounter data was processed by sensor models, and data from the sensor model was then processed by an alerting and guidance model. For this analysis, the modeled sensor was EO/IR, and the alerting and guidance algorithm was DAIDALUS. For closed-loop runs, guidance from DAIDALUS was passed to an operator model, which chose an appropriate avoidance maneuver, when necessary. For open-loop runs, the encounter dynamics were simulated without the operator model enabled. The model components depicted in Figure 3 are described, in detail, in the following paragraphs.

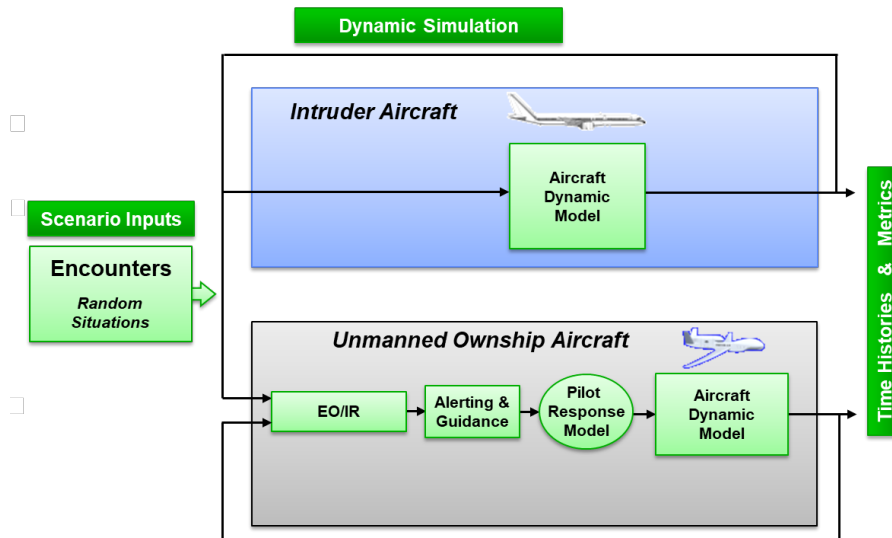


Figure 3 CASSATT simulation architecture

The EO/IR sensor model represented EO/IR sensor output by adding noise to the intruder’s truth states. The noisy intruder state and truth ownship state were input directly into DAIDALUS. The intruder was assumed to be a non-cooperative intruder that maintained its flight path during the encounter without maneuvering away from the ownship. The EO/IR sensor was integrated in the simulation environment as follows:

- 1) Used the true ownship and intruder states in the global simulation frame and calculated relative states in the ownship body reference frame (Note: no errors were applied to the ownship state).
- 2) Converted the relative states from Cartesian coordinates to spherical coordinates.
- 3) Applied the error model as described in Sections 2.1-2.4 to the relative states.
- 4) Converted the relative states with error from spherical coordinates to Cartesian coordinates.
- 5) Converted relative states back from the ownship body reference frame to the global simulation frame.

The EO/IR sensor model parameters were setup per the configurations described in Section 4.

The alerting and guidance logic in this analysis is provided by DAIDALUS, which uses state-based prediction to generate dead-reckoning trajectories for alerting and guidance computation. For this analysis, DAIDALUS was configured to have a horizontally buffered conflict volume based on the non-cooperative DAA well-clear (DWC) definition selected by SC-228. The DWC is a cylinder that has a horizontal radius of 2200 ft and a vertical distance 450 ft above and below the ownship that should not be penetrated by the intruder. Note this DWC does not have a horizontal time component. The horizontal buffer protects the ownship from sensor noise and, to some degree, unexpected intruder maneuvers. With the buffer, an alert is issued if an intruder is predicted to penetrate a cylinder around the ownship that is 3300 ft in horizontal radius, 450 ft above and below, within 60 seconds. The alert type is “Corrective” if more than 30 seconds will elapse before the intruder penetrates the buffered cylinder and “Warning” if otherwise. Corrective alerts require the pilot/operator to coordinate with air traffic control but Warning alerts allow the pilot/operator to take immediate actions to maneuver away.

For guidance computation, DAIDALUS computes heading ranges that are predicted to lead to a penetration of the ownship’s cylinder. This “conflict zone” may encompass the ownship’s current heading, prompting the pilot/operator to issue an avoidance maneuver. A turn rate of 7 deg/s, feasible for the ownship at the assumed speed range of 40 to 110 KTAS, is assumed. If the ownship does not maneuver away in time or the intruder suddenly maneuvers towards the ownship, the conflict zone may encompass the entire heading range, and no horizontal maneuvers will be able to avoid the penetration of the ownship’s cylinder. In this case, DAIDALUS continues to provide positive maneuver guidance called Well Clear Recover (WCR) bands that assists the pilot/operator to increase minimum horizontal separation as much as possible.

Vertical maneuver guidance is also computed by DAIDALUS but not selected for maneuver because

1. Non-cooperative sensors’ vertical states are usually not accurate enough to ensure robust vertical maneuvers.
2. Small to medium fixed-wing UAS’s vertical speeds are often too limited to provide effective conflict avoidance maneuvers.

The SC-228 Pilot Response Model [10] emulates the pilot/operator’s response time and maneuver selection during a DAA encounter. It assumes the pilot will coordinate with ATC if time permits (given Corrective alerts). Figure 4 shows how DAIDALUS’s alert and guidance output is processed by the pilot response model.

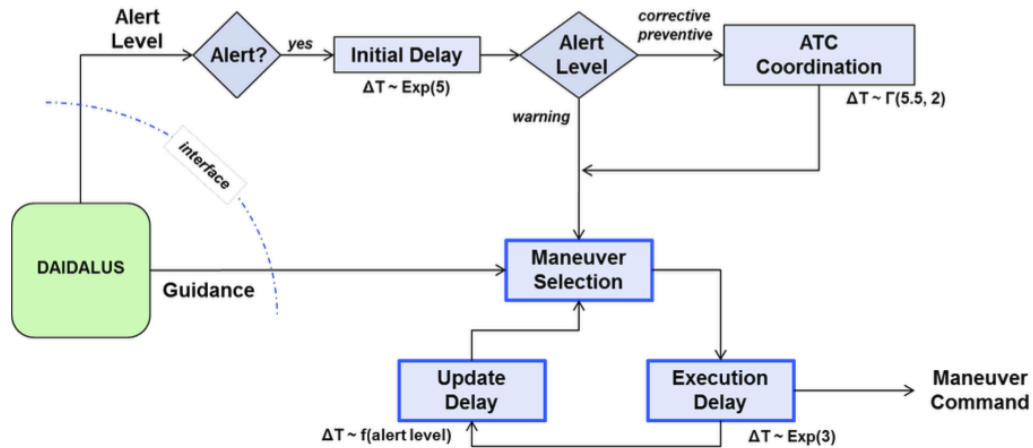


Figure 4 SC-228 pilot response model

Instead of using the delay distributions shown in Figure 4, the pilot response model was run in a deterministic mode, having a fixed 5 second initial delay, 11 second ATC coordination delay (bypassed if the alert level output by DAIDALUS is warning or above), a 3 second execution delay, and total update delays shown in Table 2. These delay times were derived from previous HITL results.

Table 2 SC-228 Pilot Model Update Delay Times

Alert Level	None	Proximate	Corrective	Warning	Recovery/WCV
Total Update Time	24 s	24 s	9 s	9 s	3 s

In addition, the pilot model was configured to:

- Issue only horizontal maneuvers

- Always turn in the direction of the minimum horizontal maneuver predicted by DAIDALUS to be conflict-free
- Add a 15° buffer on minimum suggestive horizontal guidance—a pilot behavior observed during HITLs and flight tests. Figure 5 shows how the 15° buffer is added to the edge of the conflict heading band.

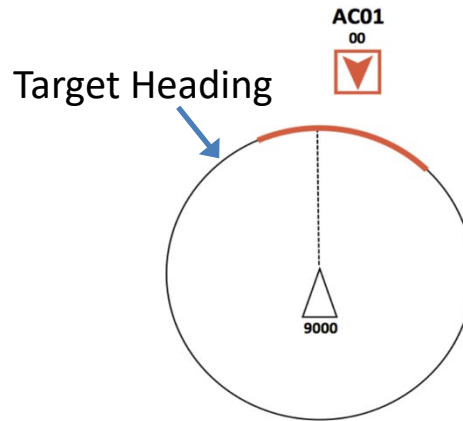


Figure 5 The pilot response model adds a 15° buffer to the edge of the conflict band

Once a DAA maneuver is selected and executed, the aircraft dynamic model deviates the ownship’s trajectory from the original heading and continues to monitor the alerts and guidance by following the data flow in Figure 3.

6 METRICS

The analysis configurations were compared using several representative DAA safety and operational suitability metrics. These metrics provide an indication of whether a system equipped with an EO/IR sensor will be able to operate safely without interfering with the operations of other aircraft and without causing DAIDALUS to alert unnecessarily. These metrics and their formulation are shown in Table 3 and Table 4.

Table 3 Safety Metrics

Metric	Notes
Risk Ratio	$\frac{P(NMAC \text{with mitigation})}{P(NMAC \text{without mitigation})}$ <p>A Near Mid-Air Collision (NMAC) occurs when the separation between two aircraft is less than 500 ft horizontally and 100 ft vertically. If the ratio is less than one, then the mitigated system reduces the risk of NMAC. For example, a risk ratio of 0.1 indicates a 90% reduction in risk. If the ratio is greater than one, then the system increases the collision risk.</p> <p>Unresolved NMAC risk is comprised of encounters that lead to nominal NMACs (i.e., without a DAA system) and which still have NMACs with the DAA system. Induced NMAC is comprised of encounters that do not have nominal NMACs but develop into NMACs with the DAA maneuver in response to DAA guidance.</p>

	A 95% confidence interval for each risk ratio was estimated through bootstrapping [11]. One hundred resamples were used to compute each confidence interval.
Loss of Well Clear Ratio	$\frac{P(\text{LoWC} \text{with mitigation})}{P(\text{LoWC} \text{without mitigation})}$ <p>Similar to risk ratio, if the Loss of Well Clear (LoWC) ratio is less than one, then the mitigated system reduces the risk of Loss of Well Clear. Unresolved and induced LoDWCs are defined in a similar way to how unresolved and induced NMACs are defined.</p> <p>A 95% confidence interval for each LoWC ratio was estimated through bootstrapping [11]. One hundred resamples were used to compute each confidence interval.</p>

Table 4 Operational Suitability Metrics

Metric	Notes
Split Alert Probability	$P(\text{Split} \text{nominal LoWC})$ <p>Splits are based off of the alert level from DAIDALUS. An encounter has a split if DAIDALUS issues an alert of any type, the alert clears, and then DAIDALUS issues another alert of any type. Additionally, in this simulation, the alert issued by DAIDALUS is put through a hysteresis filter and 2-of-4 filter (displayable alert only after at least 2 of 4 raw alerts) to improve alert operational suitability. This metric is computed using only encounters that have a nominal Loss of Well Clear (LoWC) to focus on encounters where an alert is necessary.</p> <p>Given the same risk ratio, systems with lower split alert probabilities are desirable, since fewer splits indicate greater stability in alerting.</p>
Expected Number of Split Alerts	Related to the split alert probability, this metric is presented as a probability density function (PDF). It is the distribution of the number of split alerts that occur in encounters that have a nominal LoWC. As before, distributions with lower numbers of splits are desirable.
Reversal Probability	$P(\text{Reversal} \text{nominal LoWC})$ <p>Reversals are based off of commanded headings from the pilot model. An encounter has a reversal if the commanded heading changes sign—e.g., from turn left to turn right. Note, commanded headings are always executed in the simulation. This metric is computed using only encounters that have a nominal LoWC to focus on encounters where an alert is necessary.</p> <p>Given the same risk ratio, systems with lower reversal probabilities are desirable, since fewer reversals indicate greater stability in maneuver guidance.</p>
Expected Number of Reversals	Related to the reversal probability, this metric is presented as a PDF. It is the distribution of the number of reversals that occur in encounters that have a nominal LoWC. As before, distributions with lower numbers of reversals are desirable.

Pilot Workload	$\frac{\text{Total Number of Maneuvers Performed in All Encounters}}{\text{Total Number of Encounters with a Nominal LoWC}}$ <p>Pilot workload is approximated as the average number of maneuvers performed per nominal LoWC. This metric can be interpreted as the average number of maneuvers performed per necessary alert (a nominal LoWC is considered a necessary alert condition). This numerator is computed using all encounters. Lower values are desirable.</p>
Alert Ratio	$\frac{P(\text{Alert} \text{with mitigation})}{P(\text{NMAC} \text{without mitigation})}$ <p>Given the same risk ratio, systems with lower alert ratios are desirable, since fewer alerts indicate fewer unnecessary maneuvers. Lower values are desirable.</p>

7 RESULTS

This section summarizes the aggregate metrics collected from simulating the one million encounters for all of the configurations described in Section 4.

7.1 Safety Metrics

7.1.1 Risk Ratio

Figure 6 shows the risk ratios for all of the 26 configurations that were evaluated. The percentages in the figure reflect the percentage of the baseline error (described in Section 2) used for that configuration. The following paragraphs discuss the trends observed from these configurations.

1. Default Configurations 1 to 4 (top-left subplot): The no-error configuration yields the lowest risk ratio of all configurations as expected. The default with range bias and default without range bias configurations have similar risk ratios. The 4000 ft vertical alerting threshold improves (reduces) the risk ratio to essentially the same level as the no-error result. This large vertical alerting threshold protects the ownship from both vertically blundering intruders and large vertical state uncertainties typical of non-cooperative intruders.
2. Configurations 5 to 8 (top middle) with varying angular rate errors: the risk ratio is highly correlated with increasing the angular rate error.
3. Configurations 9 to 13 (top right) with varying detection range: the risk ratio is highly correlated with decreasing the detection range when the range is below 2 NM.
4. Configurations 14 to 18 (bottom left) with varying range error: the risk ratio is insensitive to increasing the range error, even when the error is increased to four times its default value.
5. Configuration 19 to 23 (bottom middle) with varying range rate error: the same trend mostly holds for varying the range-rate error as well, except in the 400% error configuration where the risk ratio slightly increases.
6. Configuration 24 to 26 (bottom right) with simultaneously varying large range and range rate errors: the risk ratio is sensitive to scaling both the range and range-rate errors together, with errors much larger than the default sensor model configuration.

The insensitivity of the risk ratio to range and range rate error suggests EO/IR's large radial state errors may be acceptable for the DAA system. This observation, however, can be counter-intuitive at first. The explanation is the range and range rate errors affect the accuracy of the predicted time to penetration of the well clear zone for DAIDALUS. As long as the predicted time stays within the target time window for each alert type (30 to 60 seconds for Corrective and 0 to 30 seconds for Warning), pilots will not see any change in the alerting sequence.

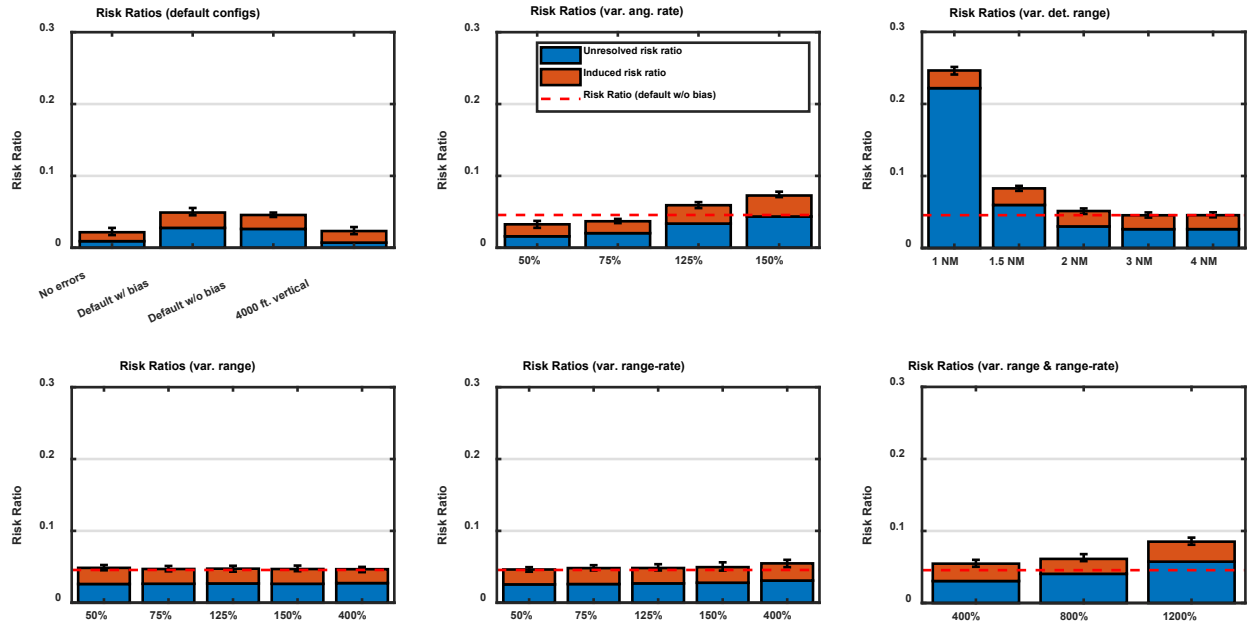


Figure 6 Risk Ratios

7.1.2 LoWC Ratio

Figure 7 shows the LoWC ratios for all of the configurations that were evaluated. The LoWC ratio follows the same trends as the risk ratios. The default with range bias and default without range bias configurations have similar LoWC ratios. The LoWC ratio is highly correlated with increasing the angular rate error and decreasing the detection range. The LoWC ratio is insensitive to increasing the range error, even when the error is increased to four times its default value. That trend mostly holds for varying the range-rate error as well, except in the 400% error configuration where the LoWC ratio slightly increases. The LoWC ratio is sensitive to increasing both the range and range-rate errors together.

7.2 Operational Suitability Metrics

7.2.1 Split Alert Probability

Figure 8 shows the split alert probability for all of the evaluated configurations. The default with range bias and default without range bias configurations have split alert probabilities close to 90%, while the no errors configuration has a split alert probability close to 30%. The 4000 ft vertical alerting threshold configuration (4) appears to reduce the split alert probability in half from the default configuration (2). The near threefold increase in split alert probability is due to EO/IR sensor noise. The effect that increasing sensor noise has on the split alert probability is also seen when the angular rate error is increased. Detection range has a more substantial effect on the split alert probability, where increasing the detection range increases the split alert probability; in these encounters, there is a larger time opportunity for the alert to split. For the variable range and variable range-rate configurations, the split alert probability is essentially saturated.

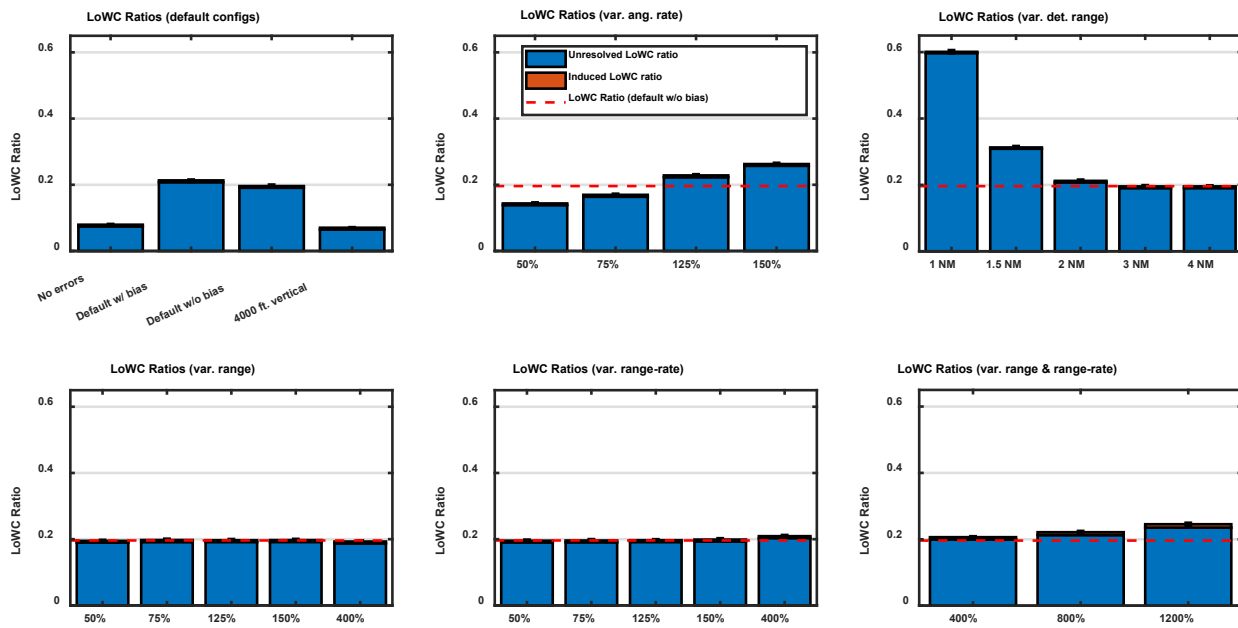


Figure 7 LoWC Ratios

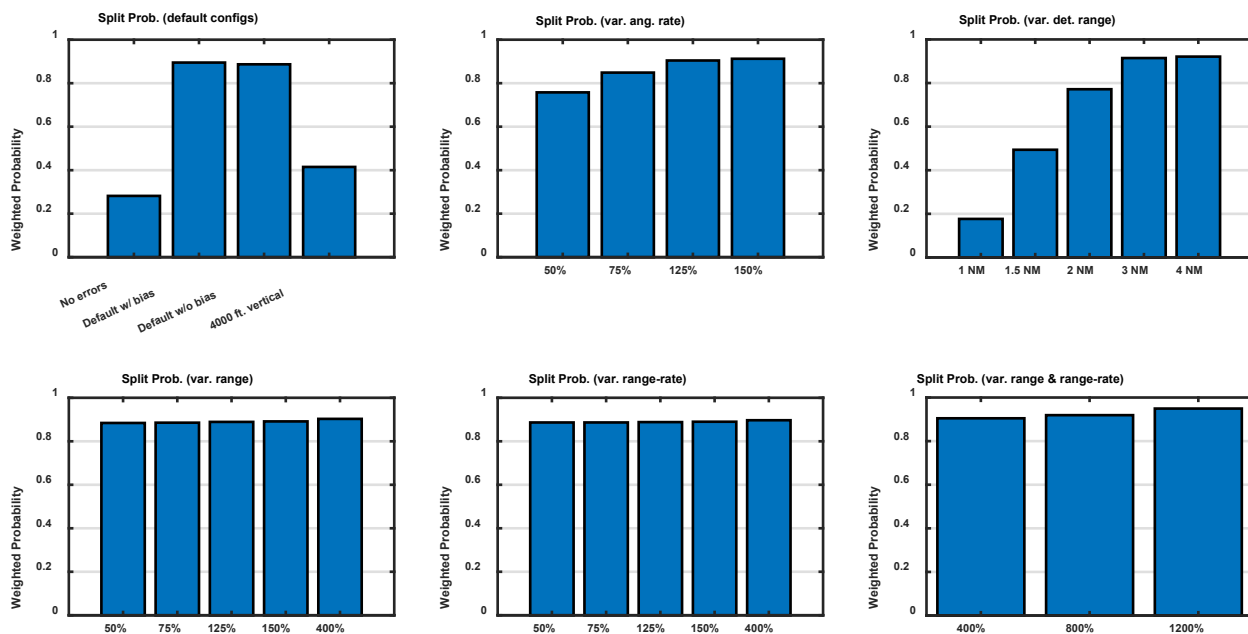


Figure 8 Split Alert Probability

7.2.2 Expected Number of Split Alerts

Figure 9 shows the probability distribution function (PDF) of the expected number of split alerts for all of the evaluated configurations. This metric was computed using only encounters that had a nominal LoWC. The dashed lines indicate the average number of splits for the configuration of the same color.

The default with range bias and default without range bias configurations have very similar distributions, showing that the range bias does not have a significant effect on the expected number of split alerts. The 4000 ft alerting threshold configuration (4) manages to keep the number of split alerts low. When the angular rate error is increased, the expected number of split alerts also increases. As the detection range increases, so does the expected number of split alerts. There is almost no variability in the expected number of split alerts for the variable range, variable range-rate and variable range and range-rate configurations.

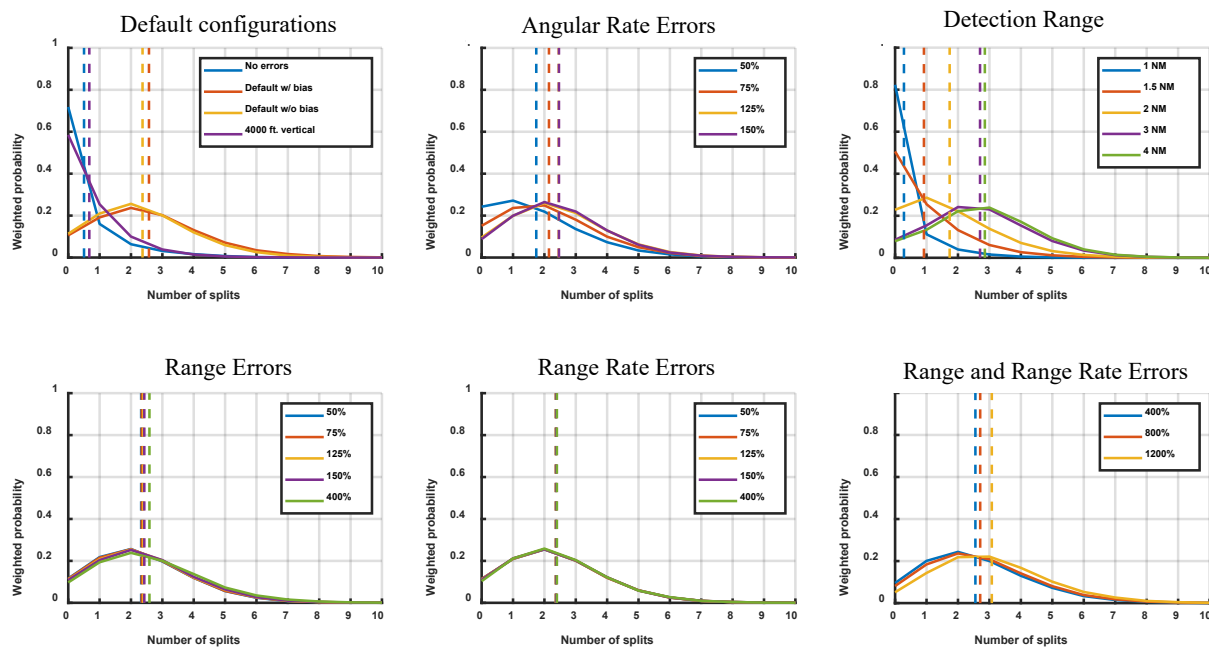


Figure 9 Expected Number of Split Alerts

7.2.3 Reversal Probability

Figure 10 shows the weighted guidance reversal probability for all of the evaluated configurations. Contrary to the split alert results, the 4000 ft vertical alerting threshold does not reduce the reversal probability from configuration 2 significantly. The guidance reversal probability is sensitive to increasing the angular rate error and decreasing the detection range below 2 NM. When the range or range-rate error is increased independently, there is an insignificant effect on the guidance reversal probability. The guidance reversal probability is sensitive to increasing the range and range-rate error together to large values.

7.2.4 Expected Number of Reversals

Figure 11 shows the weighted probability distribution of the expected number of guidance reversals for all of the evaluated configurations. This metric was computed using only encounters that had a nominal LoWC.

Note: the y-axis is zoomed to show detail. The probability distribution of guidance reversals was largely consistent among all of the evaluated configurations.

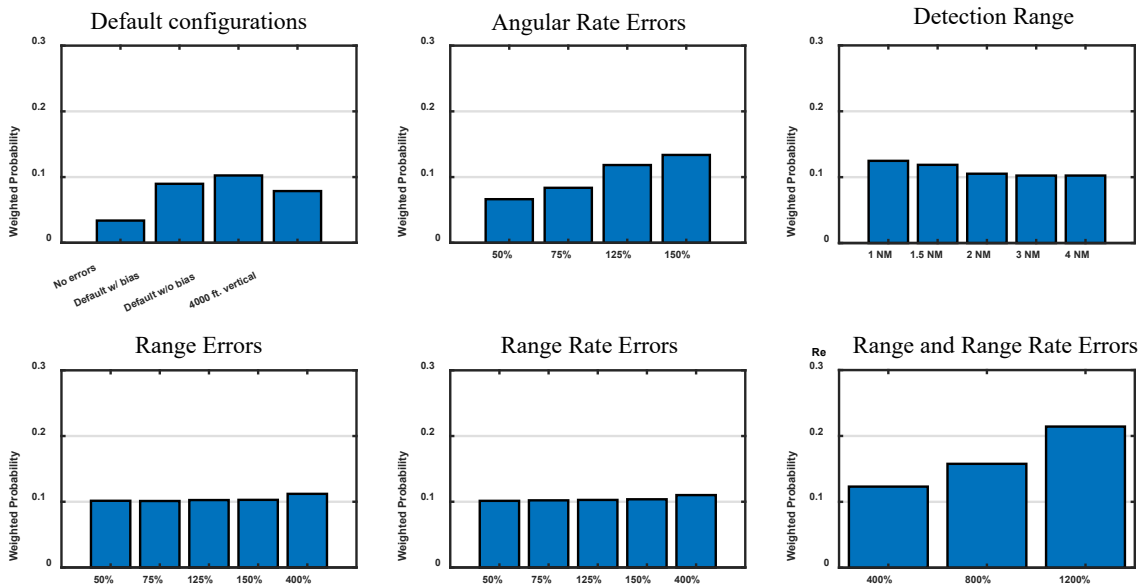


Figure 10 Reversal Probability

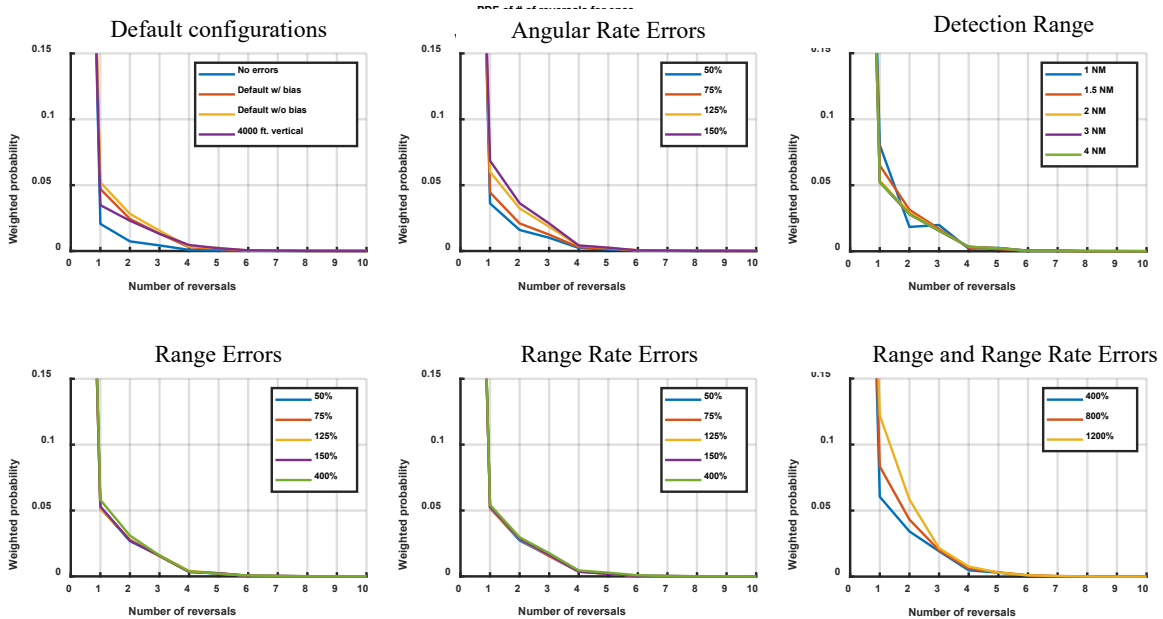


Figure 11 Expected Number of Guidance Reversals

7.2.5 Pilot Workload

Figure 12 shows the pilot workload measured by the number of alerted maneuvers performed per nominal LoWC. The default without range bias configuration performed more maneuvers than the default with range bias configuration. The 4000 ft. vertical performed almost nine maneuvers per nominal LoWC. This can be

understood as the ownship performing maneuvers even when there was not a nominal LoWC—i.e., the ownship was performing unnecessary maneuvers. The 4000 ft. vertical improves the safety metrics and split alert metric at the cost of increased pilot workload. Whether this is acceptable or not depends on additional unmodeled factors such as traffic density.

The trend follows where increasing the angular rate error degrades metric performance. Decreasing the detection range increases the number of alerted maneuvers slightly even though there is a reduced time to issue alerts. Increasing the range or range-rate error independently does not have a significant effect on the number of maneuvers performed, while increasing them together does.

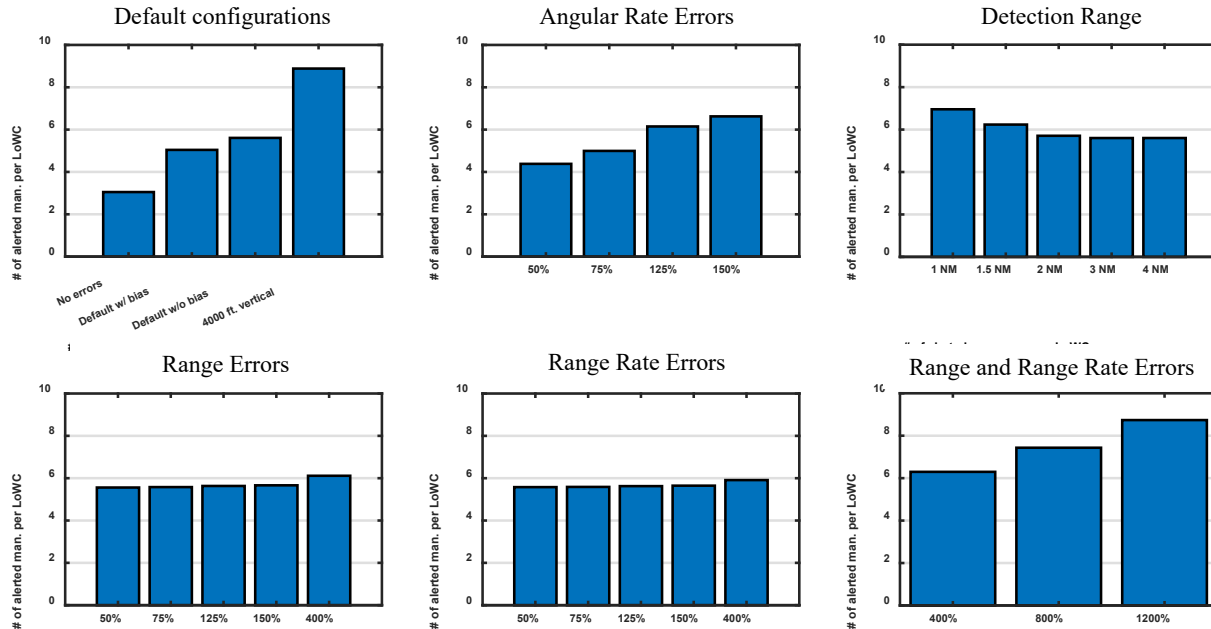


Figure 12 Pilot Workload

7.2.6 System Operating Characteristic (Alert Ratio and Risk Ratio)

The system operating characteristic (Figure 13) shows the relationship between risk ratio and alert ratio for a given configuration, which allows simultaneous evaluation of safety and operational suitability. A smaller risk ratio and alert ratio are desirable. For the default configurations, the no errors configuration had the smallest risk ratio and alert ratio, whereas the 4000 ft. vertical alerting threshold had a risk ratio similar to the no error configuration, but a larger alert ratio. For angular rate, the system operating characteristic shows a positive relationship between risk ratio and alert ratio. For detection range, there is an inversely proportional relationship between risk ratio and alert ratio. When the range error is increased beyond 400%, the alert ratio increases. Increasing the range-rate error does not significantly affect the system operating characteristic, even when the error is increased to 400% of the baseline value. When the range and range-rate error are increased together, there is only a slight increase in risk ratio but a large increase in alert ratio.

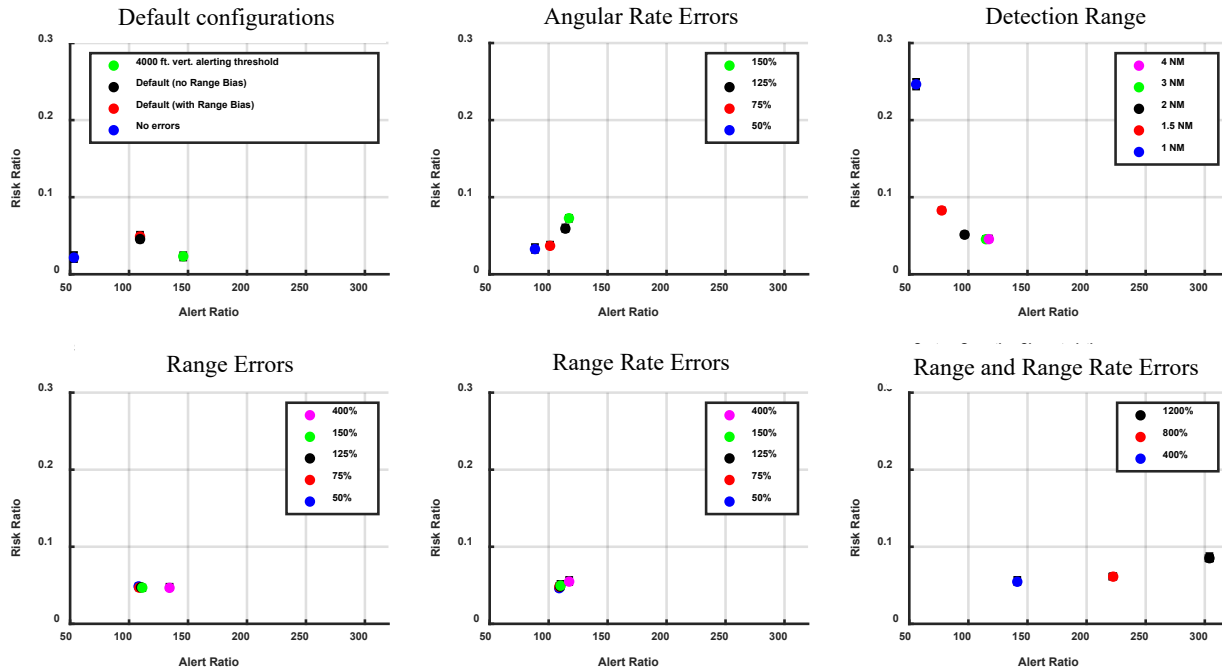


Figure 13 System Operating Characteristic

7.3 Additional Analyses

Additional analyses were performed to understand if the time correlation of a parameter could affect the metrics defined in Section 6. These analyses involved running the baseline EO/IR configuration while increasing the time correlation of a parameter and analyzing the results.

7.3.1 Increasing Angular Rate Error Time Correlation

Figure 14 shows the plots for the configurations where the angular rate error time correlation parameter (angRateTau) was increased for bearing and elevation. The baseline value of the angular rate error time correlation was 1 second. There are no noticeable effects to any of the metrics other than split alert probability, which decreased as the angular rate error time correlation was increased. This was due to the higher time correlation smoothing out the angular rate measurements.

7.3.2 Increasing Range and Range-rate Error Time Correlation

Figure 15 shows the plots for the configurations where the range and range-rate error time correlation was increased individually and together. The baseline value of the range error time correlation is 5 seconds and the baseline value of the range-rate error time correlation is 2 seconds. There are no discernable effects on the metrics from increasing the range and range-rate error time correlation.

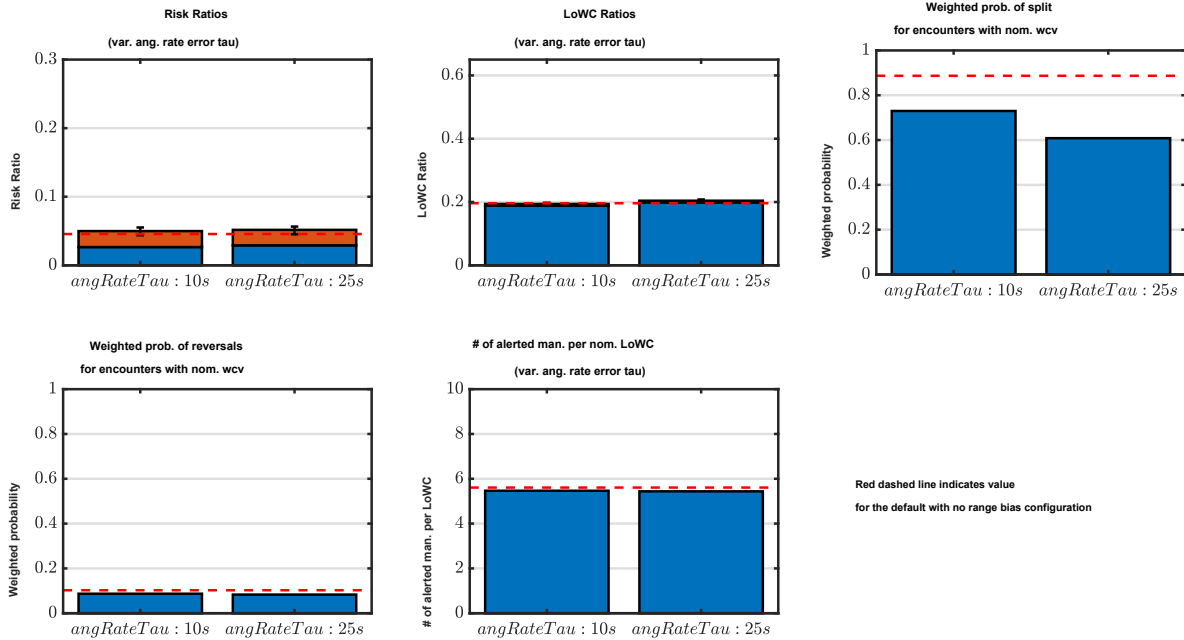


Figure 14 Metrics for variable angular rate error time correlation configurations

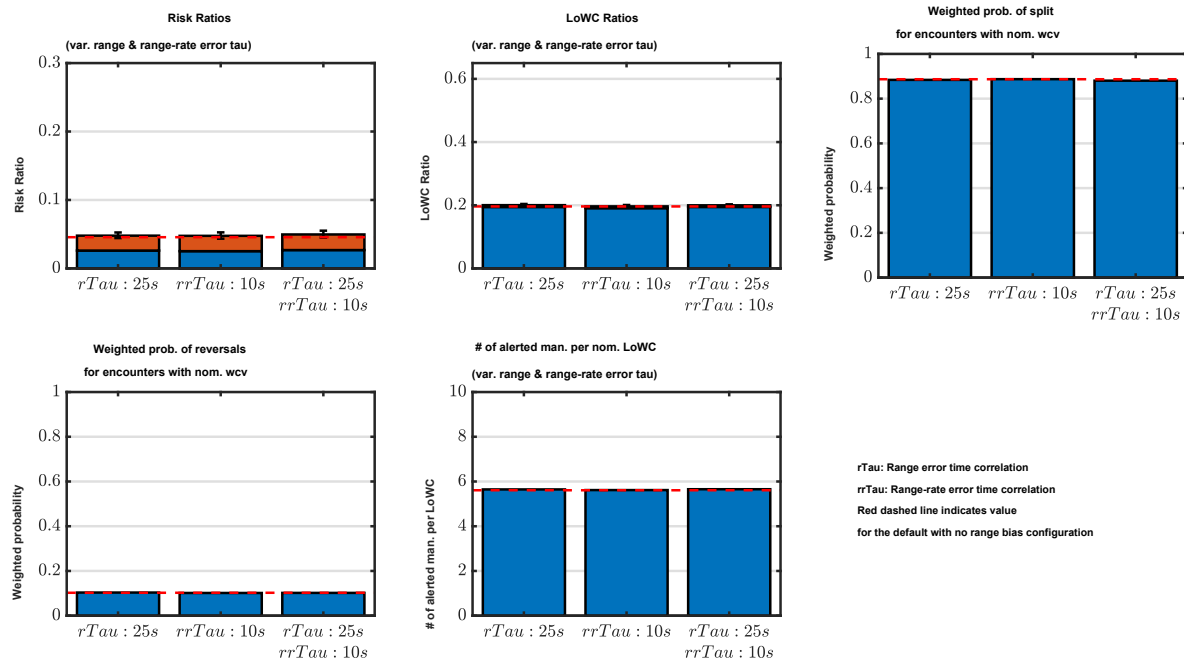


Figure 15 Metrics for Variable Range and Range-Rate Error Time Correlation Configurations

8 CONCLUSIONS AND FUTURE WORK

The results of this sensitivity analysis directly support SC-228 work on the requirements of EO/IR sensors for DAA. Analysis of the safety and operational suitability metrics shows that increasing the angular rate error and decreasing the detection range have a negative effect on DAA performance. The range and range-rate error can be increased up to four times their baseline values before DAA performance degrades. Based on these results, the minimum specification recommendations to the EO/IR MOPS are:

-
- Angular rate error: maximum $\sigma < 0.0021$ rad/s (0.12 deg/s)
 - The metrics degrade significantly when σ is 150% of the baseline sensor value (0.0014 rad/s)
 - Detection range: minimum of 2 NM
 - Decreasing detection range to below 2 NM degrades metric performance substantially. However, this analysis did not evaluate whether there was sufficient time available to coordinate with ATC, so this analysis should not be used as the sole basis to set range limits.
 - Range error: σ_r should not exceed 12% of true range
 - Performance starts to degrade when standard deviation is 400% of default (3% of true range)
 - Range-rate error: σ_{rr} should not exceed 20% of the true range-rate
 - Performance starts to degrade when standard deviation is 400% of default (5% of true range rate)

Note that, according to the Safran Electronics & Defense team, the recommended range error may not be achievable when the range is far out and close to the required detection range, which is about 2.8 NM for medium non-cooperative intruders such as a Cessna 172. The Safran Electronics & Defense team proposes an alternative range error requirement of 20% of true range for a range that is 85% of the detection range and up. An exact configuration of this condition was not tested but could be inferred from results for configurations 25 and 26. Whereas this relaxation of requirements appears to lead to very little degradation of the safety metrics, the operational suitability metrics, such as reversal probability, pilot workload, and alert ratio, are likely to be impacted by > 5%. This slight degradation was communicated to the RTCA SC-228 WG1 leadership and considered acceptable.

In addition to recommending error characteristics requirements to the EO/IR MOPS, results of the safety and operational suitability metrics for configuration 4, the 4000 ft vertical alerting threshold, demonstrate the trade space between safety and operational suitability. The increase of the alerting volume in the vertical dimension improves the safety metrics significantly by protecting the ownship from vertical state noises and vertically blundering intruders. This increased alerting volume, however, leads to considerably more pilot workload in terms of number of executed maneuvers. This trade-off should be reasonable in low traffic density areas with low encounter rate but may be problematic in the presence of medium to high traffic density.

The approach laid out in this analysis is general and can be applicable or easily adaptable to analysis of other types of DAA sensors such as acoustic sensors or ground-based surveillance systems. DAIDALUS allows users to turn on the Sensor Uncertainty Mitigation (SUM) [13] function that can take into account surveillance errors in its alerting and guidance computation. It would be interesting to assess the effectiveness of SUM in mitigating the effect of EO/IR sensors' noise on DAA systems in future work.

REFERENCES

- [1] RTCA SC-228, DO-365B, Minimum Operational Performance Standards (MOPS) for Detect and Avoid (DAA) Systems, RTCA Inc., 2021.
- [2] SAFRAN Electronics and Defence, "White Paper for the EO/IR Sensor Model," RTCA SC-228, 2019.

-
- [3] "Appendix Q," in *Minimum Operational Performance Standards (MOPS) for Detect and Avoid (DAA) Systems*, DO-365, RTCA. Inc., 2017.
- [4] RTCA SC-228, DO-366A, Minimum Operational Performance Standards (MOPS) for Air-to-Air Radar for Traffic Surveillance, RTCA, 2020.
- [5] M. G. Wu, S. Lee, C. Serres, B. Gill, M. W. M. Edwards, S. Smearcheck, T. Adami and S. Calhoun, "Detect-and-Avoid Closed-Loop Evaluation of Noncooperative Well Clear Definitions," *Journal of Air Transportation*, vol. 28, no. 4, pp. 195-206, October 2020.
- [6] K. J. Monk, J. Keeler, R. C. Rorie, G. Sadler and C. Smith, "UAS Pilot Performance Comparisons with Different Low Size, Weight and Power Sensor Ranges," in *2020 AIAA/IEEE 39th Digital Avionics Systems Conference (DASC)*, 2020.
- [7] S. Ayyalasomayajula, R. Sharma, W. F. A. Trani, N. Hinze and S. Spencer, "UAS Demand Generation Using Subject Matter Expert Interviews and Socio-Economic Analysis," in *Proceedings of the AIAA Aviation Conference*, 2015.
- [8] A. Weinert, E. Harkleroad, J. Griffith, M. Edwards and M. Kochenderfer, "Uncorrelated Encounter Model of the National Airspace System Version 2.0 (ATC-404)," Lincoln Laboratory, Lexington, MA, 2013.
- [9] A. Nuic, D. Poles and V. Mouillet, "An Advanced Aircraft Performance Model for Present and Future ATM Systems," *International Journal of Adaptive Control and Signal Processing*, Vol. 24, No. 10, pp. 850-866, 2010.
- [10] C. Muñoz, A. Narkawicz, G. Hagen, J. Upchurch, A. Dutle, M. Consiglio and J. Chamberlain, "DAIDALUS: Detect and Avoid Alerting Logic for Unmanned Systems," in *34th IEEE/AIAA Digital Avionics Systems Conference*, Prague, Czech Republic, 2015.
- [11] MIT Lincoln Laboratory, "A Model of Unmanned Aircraft Pilot Detect and Avoid Maneuver Decisions," MIT Lincoln Laboratory, 2017.
- [12] B. Efron, "Better Bootstrap Confidence Intervals," *Journal of the American Statistical Association*, vol. 82, no. 397, pp. 171-185, 1987.
- [13] A. Narkawicz, C. Muñoz and A. Dutle, "Sensor Uncertainty Mitigation and Dynamic Well Clear Volumes in DAIDALUS," in *Proceedings of the 37th Digital Avionics Systems (DASC 2018)*, London, England, 2018.